

Development of Synoptic-Scale Disturbances over the Summertime Tropical Northwest Pacific

ADAM H. SOBEL AND CHRISTOPHER S. BRETHERTON

Department of Atmospheric Sciences, University of Washington, Seattle, Washington

(Manuscript received 29 April 1998, in final form 24 November 1998)

ABSTRACT

This study addresses the origin of the synoptic-scale disturbances that occur in the tropical western North Pacific ocean (WP) region in Northern Hemisphere summer. These have been called “easterly waves” and “tropical depression-type” (TD) disturbances. This analysis uses the National Center for Environmental Prediction–National Center for Atmospheric Research reanalysis dataset. By performing a regression analysis on several terms in the vorticity equation at 850 hPa, it is shown that the TD disturbances propagate approximately as barotropic Rossby waves at 850 hPa. Given this, ray-tracing calculations and the wave activity diagnostic introduced by Plumb are used to show that wave accumulation is a promising candidate for the initial development mechanism of the TD disturbances. The expected local “growth rate” from this mechanism is simply the convergence of the group velocity, which reaches values corresponding to a growth timescale of 3 days. This convergence is dominated by, but somewhat larger than, the convergence in the time-mean flow. The wave accumulation mechanism can operate either on waves coming from outside the WP region or on those generated in situ; in particular, mature tropical cyclones are probably a climatologically important source of waves. While the results presented here provide no direct information on the nature of the feedbacks between diabatic processes and large-scale wave dynamics, they do indicate that no *linear* instability mechanism involving any diabatic process need be invoked to explain the initial development of TD disturbances. It is possible, rather, that diabatic processes do not provide a positive feedback until the disturbances reach finite amplitude, whether at the stage of true tropical cyclogenesis or some prior intermediate stage.

1. Introduction

We address here the origin of the synoptic-scale disturbances observed in the tropical western North Pacific ocean region [referred to hereafter as the WP region, following Lau and Lau (1990)] in Northern Hemisphere summer. These have been generally referred to as “easterly waves,” or more recently as “tropical depression-type” (TD) disturbances (Takayabu and Nitta 1993; Dunkerton and Baldwin 1995); the latter terminology will be preferred here.

We exclude from detailed discussion Atlantic easterly waves, sometimes referred to as “African waves.” We also exclude the mixed Rossby-gravity (MRG) mode, which to some extent coexists with the TD mode in the WP region. Generally, these two modes can be distinguished from each other by several different characteristics. The MRG mode has longer wavelengths and faster phase speeds than the TD mode, and the MRG mode is generally observed to be dominant over the central

Pacific, whereas the TD mode dominates over the WP region (Wallace 1971, and references therein; Liebmann and Hendon 1990; Takayabu and Nitta 1993; Dunkerton and Baldwin 1995). The MRG mode is a true equatorial mode, whereas the TD mode is both observed primarily off the equator and has dispersion properties that do not appear consistent with any linear equatorial mode (Liebmann and Hendon 1990; Takayabu and Nitta 1993; Takayabu 1994). The TD mode is predominantly lower tropospheric, though sometimes deepening to fill the troposphere. MRG modes seem to exist both in the upper and lower tropospheres, without there necessarily being any connection between the two (Wallace 1971, and references therein; Dunkerton and Baldwin 1995). The TD mode is more tightly coupled to convection than is the MRG mode (Takayabu and Nitta 1993; Dunkerton and Baldwin 1995).

Disturbances of TD type have also been observed in the eastern North Pacific (e.g., Tai and Ogura 1987; Lau and Lau 1990; Ferreira and Schubert 1997; Molinari et al. 1997; Raymond et al. 1998). These will be discussed here only tangentially. Hereafter, unless stated otherwise, our discussion refers to the WP region.

The existence and general characteristics of TD disturbances have been known to some extent since at least

Corresponding author address: Dr. Adam H. Sobel, Department of Atmospheric Sciences, University of Washington, Box 351640, Seattle, WA 98195-1640.
E-mail: sobel@atmos.washington.edu

the 1940s (e.g., Riehl 1948). A number of detailed and quantitative studies were performed, using primarily spectral analysis techniques applied to island station data in the late 1960s and early 1970s. A comprehensive review of these is given by Wallace (1971). The compositing study of Reed and Recker (1971) provided a particularly clear view of the disturbances' structure and some aspects of their dynamics. A number of observational studies have been performed on these disturbances in more recent years (Nitta and Takayabu 1985; Lau and Lau 1990, 1992, hereafter LL90, LL92; Liebmann and Hendon 1990; Heta 1991; Takayabu and Murakami 1991; Dunkerton 1993; Takayabu and Nitta 1993; Dunkerton and Baldwin 1995).

It is still unclear how the TD disturbances are generated. This stands in contrast to the Atlantic case, in which it is fairly clear that the waves are generated over Africa due to the shear instability of the easterly jet [for a recent review, see Thorncroft and Hoskins (1994)]. The eastern North Pacific (hereafter EP) has been the subject of some recent interest, with a prominent hypothesis being the barotropic instability of the inter-tropical convergence zone (ITCZ). This mechanism was suggested by Charney (1963), Nitta and Yanai (1969), and in much greater detail by Schubert et al. (1991) and Ferreira and Schubert (1997). This mechanism appears less likely to be applicable in the WP, as discussed further below. Molinari et al. (1997) propose a related hypothesis for the EP, that barotropic instability occurs in the Caribbean Sea, and the waves then propagate into the EP. Mozer and Zehnder (1996) have proposed that flow past the Sierra Madre in Mexico may provide a mechanism for the development of the EP disturbances.

In the WP region, there is at least an equally large uncertainty about the development mechanism for the TD disturbances, and less recent attention to the problem. A number of observational studies have documented positive correlations among diabatic heating, temperature, and vertical velocity in the upper troposphere, and inferred from this that the waves are maintained through latent heat release associated with cumulus convection (Nitta 1970, 1972; Reed and Recker 1971; Kung and Merritt 1974; LL90; LL92). We will argue below that this mechanism may in some of the studies be overemphasized, due to the fact that mature tropical cyclones are mixed in with the weaker TD disturbances by certain data analysis techniques. (Here, by "mature tropical cyclone" or "tropical cyclone" we intend to denote a disturbance characterized by a particular type of dynamics rather than any particular threshold value of some observable quantity. It is not clear beyond all doubt in all cases exactly at what stage of development true tropical cyclone dynamics is active. By default, we can choose the standard definition of sustained surface winds larger than 17 m s^{-1} . However, as only statistical aggregates of disturbances will be explicitly discussed here, a precise definition of this sort will not be specifically necessary.) Furthermore, even

if the disturbances are maintained by convection, this neither sheds light directly on their initiation nor gives us any particularly clear insight into how the convection and synoptic-scale disturbance dynamics feed back upon each other such as to produce this result.

From a theoretical perspective, a number of mechanisms have been proposed to explain the TD disturbances. Holton (1971) used a diagnostic model to study the atmosphere's response to prescribed patterns of diabatic heating. This provided an explanation for the variations in vertical structure observed in different parts of the domain, due to the corresponding variations in mean vertical shear. However, since the heating is prescribed, this model does not constitute a complete theory of the disturbance dynamics. Later theories for TD waves have gone further, by internalizing assumptions about the feedbacks between diabatic processes and the synoptic-scale flow. Stevens et al. (1977) and Stevens and Lindzen (1978) invoked a version of the conditional instability of the second kind (CISK) hypothesis, while Emanuel (1993) invoked wind-induced surface heat exchange (WISHE). Both of these involve convection, but they posit different views of the way in which convection interacts with the mean flow, as discussed broadly by Emanuel et al. (1994).

Both mechanisms do, however, formulate the problem in terms of a linear instability in which a feedback between diabatic processes and wave dynamics is essential to the initial disturbance growth, though Stevens et al. (1977) and Stevens and Lindzen (1978) offer an interpretation in which the linearization of their CISK model is portrayed explicitly as a mathematical convenience more than, necessarily, a correct physical description. WISHE is also well known as a nonlinear mechanism in the formation and maintenance of mature tropical cyclones, as in Rotunno and Emanuel (1987), but Emanuel (1993) studied linear WISHE modes.

We will argue that an entirely different mechanism is likely to be important. This is the accumulation of Rossby wave activity [as defined by Plumb (1986)], due mainly to the convergence of the low-level mean flow in the WP region. The mechanism of Rossby wave accumulation has been studied in broad theoretical terms by Farrell and Watterson (1985). Essentially this mechanism was invoked earlier, though using somewhat different language, to explain Atlantic tropical cyclogenesis from preexisting easterly waves by Shapiro (1977). Variants of the same mechanism, involving both Rossby and other sorts of waves (i.e., equatorial modes), have been studied by Zangvil and Yanai (1980), Yanai and Lu (1983), Webster and Chang (1988), and Chang and Webster (1990, 1995). However, to the extent that they have explicitly addressed specific observed phenomena, the latter studies have focused primarily on the upper troposphere, in some cases only during the winter season, with attention paid also to tropical-midlatitude interactions. To our knowledge, the first, and so far only, study that has pointed out the likely importance of this

mechanism in the *lower* troposphere, in the summertime WP region, is that of Holland (1995). Here, we present more concrete and quantitative evidence for the importance of this mechanism.

Our argument has two parts. The first is that the TD disturbances propagate approximately as layerwise barotropic Rossby waves at 850 hPa. This does not necessarily imply that they are pure Rossby waves as far as their energetics are concerned, only that any other mechanism that affects their amplitude has, at most, a weak effect on their propagation characteristics. This conclusion corroborates Holton (1970), who argued on grounds somewhat different from ours that the disturbances are forced, equatorially trapped Rossby waves (though our analysis does not assume or require equatorial trapping). It is also broadly consistent with observational studies that are more methodologically comparable to ours, of Atlantic easterly waves (Shapiro 1978; Stevens 1979) and similar Southern-Hemispheric tropical disturbances (Davidson and Hendon 1989) if we assume that conclusions about the propagation mechanisms of the disturbances in these regions are relevant to those in the WP region, and with LL92, whose results are directly relevant to this question for the TD modes in the WP region.

The nearly barotropic, nondivergent propagation recalls the scaling argument of Charney (1963) [see also the discussion in Holton (1992)] who indicated that synoptic-scale tropical disturbances *in the absence of moisture condensation* should be nondivergent and obey a barotropic vorticity equation to leading order. It is interesting that Charney's prediction seems to hold to a significant extent, even though there is substantial moisture condensation associated with the TD disturbances.

The second part of the argument is that, given that the disturbances propagate as barotropic Rossby waves, these waves converge in the WP region, leading to an accumulation of wave activity there. This is to be expected, as pointed out by Holland, simply because the lower-level mean flow converges. However, our calculations provide more concrete support for this view, including an estimate of the typical local growth rate that one expects by this mechanism. Over a region of synoptic-scale extent, this growth rate reaches a value of $3 \times 10^{-6} \text{ s}^{-1}$ (corresponding to a timescale of around 3 days). This is large enough to be competitive with any plausible dissipation mechanism, leading us to the conclusion that this mechanism is indeed important.

It should also be said at the outset that while the mechanism discussed in this paper provides a plausible explanation for why and how TD disturbances experience initial growth where they do, it does not explain other important observed features, such as their wavelength and interaction with atmospheric convection.

2. Data

a. Basic dataset

The data used are the National Center for Environmental Prediction–National Center for Atmospheric Re-

search (NCEP–NCAR) reanalyses (Kalnay et al. 1996), from the years 1985–96. We have used the version of this dataset that is available on CD-ROM; this contains twice-daily wind fields at 850, 500, and 200 hPa (among other quantities). The present study uses explicitly only these wind fields and quantities (such as vorticity) that can be derived from them. We have selected the period from 15 May to 15 September of each year for analysis. Tropical cyclone track data from the Joint Typhoon Warning Center were used to identify named tropical cyclones in Figs. 4 and 11.

b. Time filter

In many of the calculations presented below, we digitally bandpass filter various quantities in time to isolate synoptic frequencies. The filter has full power between 2 and 6 days and falls to half-power at 1.5 and 11.5 days. This is a relatively broad filter, intended to leave as much signal as possible while still removing the diurnal cycle and slow intraseasonal variability such as that associated with the Madden–Julian oscillation.

c. Climatological fields

Figure 1 shows the time-mean wind and absolute vorticity fields over the entire data record, at 850, 500, and 200 hPa. The 850-hPa wind field is very similar to that shown in Fig. 2 of LL90, indicating consistency between the NCEP–NCAR reanalyses and the European Centre for Medium-Range Weather Forecasts (ECMWF) operational analyses that LL90 used, at least in this aspect of the climatology.

At 850 hPa, note that the mean flow has a large component across the mean vorticity contours in the western part of the domain, around 120° – 140° E. The instantaneous low-level winds vary strongly from the time-mean picture, on intraseasonal as well as shorter and longer timescales. The general character of westerlies meeting easterlies somewhere near the monsoon trough region is always present, but bands of westerlies appear rather variably both in the latitude at which they are centered and the degree to which they extend eastward. As a rule, though, the eastward extent of the lower-level westerlies decreases with increasing altitude in the lower troposphere, as can be seen by comparing the mean winds at 500 and 850 hPa in the western end of the domain shown in Fig. 1. The causes and significance of the low-level monsoon westerlies are discussed by Holland (1995); their role in TD disturbance dynamics, in particular, is considered further below.

In the calculations in sections 4 and 5, we will consider the TD waves as propagating on the climatological time-mean flow. Because of the intraseasonal variability, this is somewhat inaccurate. However, the most important feature of the mean flow will be its strong zonal convergence, and this is essentially always present with comparable magnitude even in instantaneous fields,

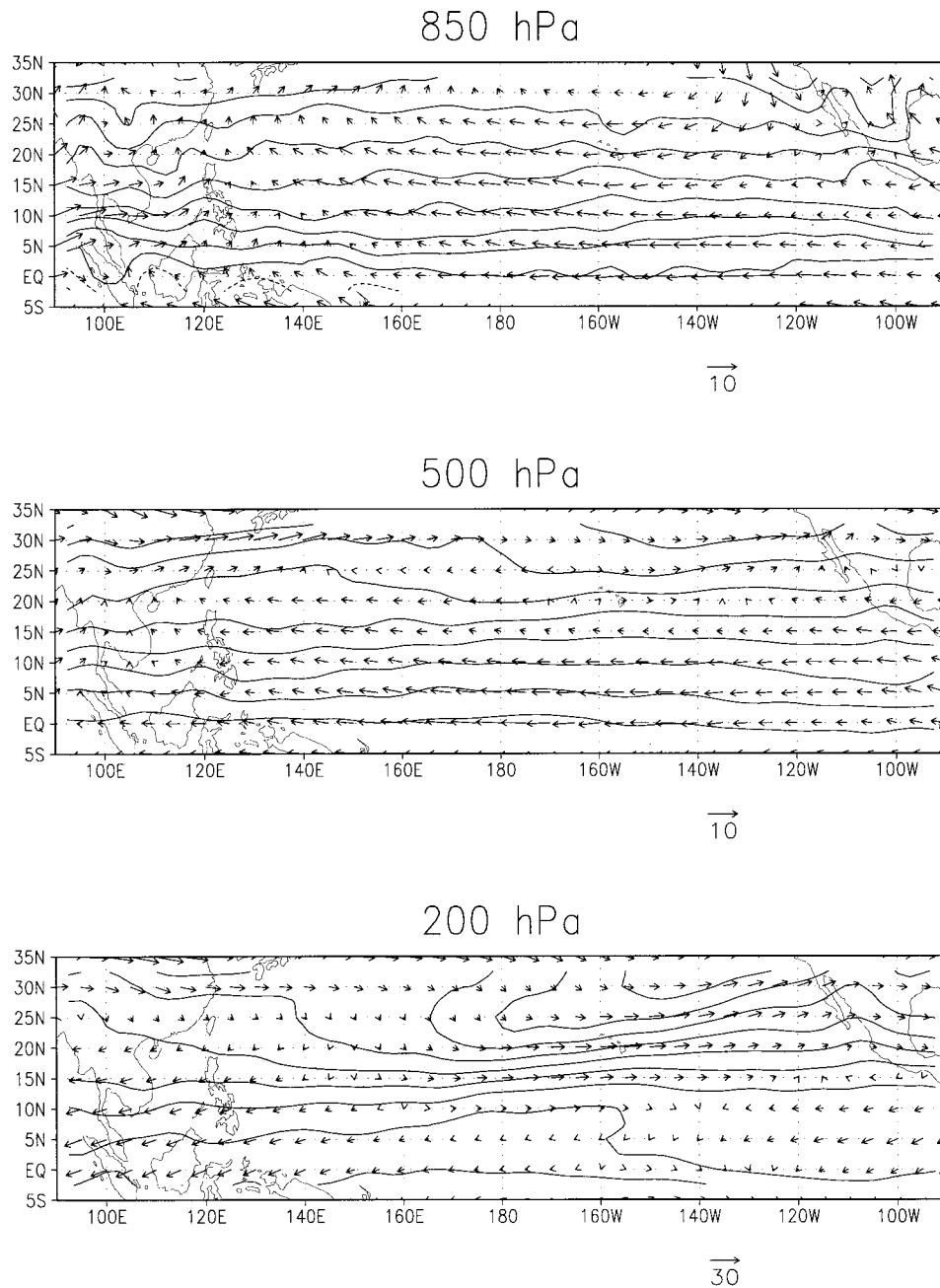


FIG. 1. Climatological mean wind (m s^{-1}) and vorticity (s^{-1}) fields from the NCEP–NCAR reanalyses at 850, 500, and 200 hPa. Vorticity contour interval is 10^{-5} s^{-1} .

though the location where it maximizes varies to some extent. Hence, considering the waves as propagating on the mean state shown in Fig. 1, while something of a distortion, should not lead to incorrect conclusions at the level of accuracy we attempt.

Broadly, with the notable exception of the tongue of high vorticity extending southwestward from midlatitudes into the subtropics at 200 hPa, which we interpret as the time-mean tropical upper-tropospheric trough (Sadler 1976), the time-mean absolute vorticity fields

at all three levels are rather zonal and uninteresting. For most purposes, one would not go very wrong by assuming that the absolute vorticity gradient simply equals its planetary component. This is a preliminary indication that barotropic instability of the ITCZ is not an important process here, since we see no sign reversal or region of homogenized vorticity. Though we do not show it here, the same would be true if we showed Ertel potential vorticity (PV) on lower-tropospheric isentropes (this field is included on the NCEP–NCAR reanalysis

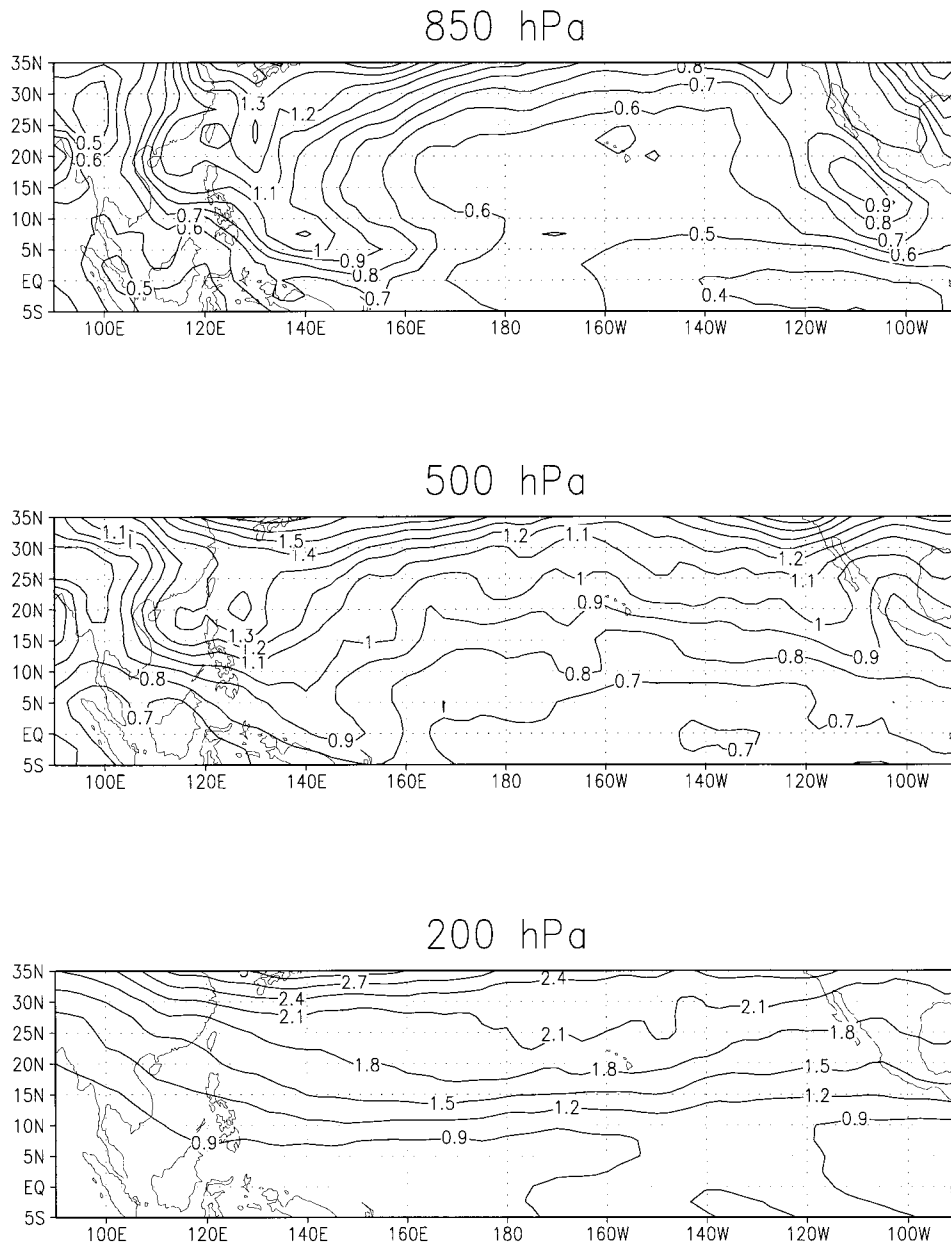


FIG. 2. Standard deviation of bandpassed vorticity at 850, 500, and 200 hPa (10^{-5} s^{-1}).

CD-ROMs), though the increase in dynamical significance of (dry) PV over absolute vorticity is in any case questionable in a moist convective regime. The same is also true of time-mean fields (for either quantity) over single seasons or single months.

d. Barotropic instability and ITCZ breakdown

Of course, if barotropic instability were an important factor, one would not necessarily expect to observe the unstable state in the time mean, as the unstable disturbances would continually act to remove the instability. Though there is no way of presenting this information

here, we have repeatedly watched animations of absolute vorticity at 850, 500, and 200 hPa for several seasons.¹ One virtually never unambiguously sees a strip of vorticity form and then break up into waves or vortices, as in the simulations of Ferreira and Schubert (1997), anywhere in the tropical Pacific. When there is

¹ It is, however, fairly easy for the interested reader to obtain, at low cost, the NCEP-NCAR reanalysis CD-ROMs, which include the program GrADS. With this program, it is extremely easy to make color animations of the data, so the reader can, with little effort, form his or her own impressions of the phenomenology we describe.

something like a strip present, it has virtually always formed through the merger of several preexisting vortices, the *opposite* sequence of events.

On the other hand, it could be that a PV or vorticity sign reversal occurs in a layer that is thin in the vertical, so that we miss it by looking only at the 850- and 500-hPa fields, or that the data are otherwise inadequate to reveal the sign reversal. This is relatively plausible in the EP, since infrared cloud images at least show strip-like structures there [cf. Fig. 1 of Ferreira and Schubert (1997)]. Furthermore, the EP is data poor even by tropical ocean standards, so the reanalysis data are mostly model generated and hence not particularly trustworthy in the EP.²

By contrast, in infrared cloud pictures of the WP region, one very rarely observes sequences of the sort shown in Fig. 1 of Ferreira and Schubert. This lack of a clear ITCZ in the WP, a trait that distinguishes it from most other tropical regions, was noted as early as half a century ago by Riehl (1948). The WP is also relatively well sampled by the observational network (by tropical ocean standards). Therefore, whatever the validity of the barotropic instability hypothesis in the EP, it seems unlikely to explain the development of TD disturbances in the WP. Nitta and Yanai (1969) argued that there was, in fact, a barotropically unstable ITCZ around the Marshall Islands, with maximum disturbance growth rate corresponding to a timescale of 5 days. However, their analysis showed a mean vorticity gradient sign reversal only at the surface and 1000-hPa levels, suggesting that substantial dissipation should be included in the stability calculation to represent surface drag, but their calculation was inviscid. Further, their mean state was derived solely from Marshall Islands station data, so that it represents explicitly only a very limited longitudinal range, rather than a strip (of greater than a TD wavelength) per se. Summertime seasonal calculations of vorticity using the 10-m winds in the NCEP–NCAR reanalyses (not shown) show no gradient sign reversal in the WP region.

The study of LL92 indicated a significant degree of conversion of barotropic mean flow energy to disturbance energy. This is not inconsistent with our argument that the ITCZ breakup mechanism is inapplicable to the WP region, as long as the conversion is nonmodal. In this case the barotropic conversion is subsumed into the wave activity convergence mechanism. This is discussed further in the concluding discussion.

3. Vorticity and propagation dynamics from regression analysis

a. Technique

To study the vorticity and propagation dynamics of the disturbances, we use the regression analysis technique

introduced by Lim and Wallace (1991). This technique is, in turn, a modification of those used in the earlier studies of Blackmon et al. (1984a,b) and Wallace et al. (1988). One first constructs a reference time series by dividing the time series of some variable at a fixed point by its standard deviation. Then any variable, evaluated at all grid points, is regressed against the reference time series to obtain a regression coefficient that has units of the regressed variable. This coefficient forms a sort of composite field that is associated statistically with a perturbation in the reference variable of one standard deviation. In most applications of this technique, the reference time series is subjected to some form of time filtering in order to isolate fluctuations of some particular timescale. The regressed variable may or may not be time filtered. Treatments of various issues associated with time filtering, and more detailed discussions generally of this technique, can be found in Lim and Wallace (1991) and Chang (1993).

A similar regression technique (the computation of dimensionless correlation coefficients) was used by LL90 to illuminate certain basic aspects of easterly waves. LL90 also used a compositing technique based on extended empirical orthogonal functions (EEOFs). Our analysis is less comprehensive than theirs, but also differs from theirs in several other respects. We use a different dataset and focus particularly on the issue of what determines the phase velocity (and implicitly, also the group velocity) of the waves. We use the Lim and Wallace (1991) regression technique to produce a composite vorticity equation in order to address this issue.

LL92 performed detailed analyses of the energetics, as well as propagation and vorticity dynamics of TD waves, using the EEOF compositing technique of LL90 (with the exception that LL90 filtered the data in time before the compositing, while LL92 did not; this difference had little effect on the results). The LL90–LL92 compositing technique and the simpler regression technique both yield results that may be to some extent affected by mature tropical cyclones, since these have roughly the same space scales and timescales (and indeed, in other respects as well, similar structures) as TD disturbances.³ However, the compositing technique of LL90 and LL92 may be even more prone to contamination by tropical cyclones, since this technique particularly selects episodes of large variance in 850-hPa vorticity (as projected on the leading EEOFs) and throws away periods of smaller variance. The simpler regression technique at least keeps all the data, though it is still weighted by disturbance amplitude, as reflected in

² However, Tai and Ogura (1987) performed a study of the EP using FGGE level III-b data, and also found no evidence of barotropic instability.

³ Tropical cyclones are often considered to be mesoscale phenomena, as opposed to the synoptic-scale TD disturbances. However, typical statistical analysis techniques are more sensitive to the spacing between cyclones than to the size of the main cyclone circulation itself. The typical spacing between tropical cyclones is better described as synoptic than as mesoscale.

the reference time series. Additionally, the LL90–LL92 composites focused on the northwestward end of the typical “storm track” of the disturbances, as opposed to, for example, Reed and Recker (1971), who focused more on the region around the Marshall Islands, where the disturbances appear to develop initially (e.g., Takayabu and Nitta 1993). This can also be expected to increase the influence of tropical cyclones, since cyclogenesis typically occurs after an initial disturbance has propagated somewhat northeastward.

While neither LL90 nor LL92 mentioned this issue, Lau’s (1991) doctoral dissertation, which presented essentially the same research as those two papers but with some additional information, examined it in some detail. Lau’s conclusion was that mature tropical cyclones did have some influence on the composites, but that the wavelike structure observed was nonetheless a real feature (i.e., of the relatively weaker TD disturbances), rather than being simply an artifact of passing tropical cyclones through a bandpass filter. Our results here, as well as previous studies, provide additional evidence in agreement with this conclusion. However, this still leaves open the possibility that more subtle aspects of the LL90–LL92 studies, such as the energetics of the disturbances, may have been distorted by the influence of tropical cyclones. For one, since we expect the latter to exhibit correlations among heating, vertical velocity, and temperature, this signature in the composites may be overemphasized relative to what actually occurs in noncyclogenetic or precyclogenetic TD disturbances.

To minimize the effect of tropical cyclones on our results, we pay more attention to the southeastward than the northwestward region of the TD disturbance storm track, and use regression rather than a technique such as that of LL90–LL92. Takayabu and Nitta (1993) and Dunkerton and Baldwin (1995) also used regression techniques to study the same disturbances, but their results do not directly address the question of what determines their phase speed, while those of LL92 do, since the latter constructed an explicit composite vorticity equation.

Following LL90–LL92 we use relative vorticity at 850 hPa as our reference time series. Both the reference time series and all quantities that are regressed against it are filtered in time as described in the previous section.

b. Basic patterns

Figure 2 shows maps of the standard deviation of time-filtered vorticity at 850, 500, and 200 hPa. The map at 850 hPa is very similar to the upper panel of Fig. 1 in LL90, who plotted the same quantity, though using a different time sample, dataset, and no time filtering. The similarity is encouraging as far as it reinforces our general confidence in gridded analysis products in this region. The fact that the presence or absence of time filtering makes little difference indicates simply that most of the variance in 850-hPa vorticity occurs at

synoptic frequencies (as we have verified by producing the same plot, not shown, with unfiltered data). The tongue of high variance that extends southeastward from the southern coast of China defines what we mean by the storm track for TD disturbances (as well as tropical cyclones).

The 500-hPa map looks fairly similar to the 850-hPa one, though the tongue of large variance extends farther south. The 200-hPa map shows no sign of this tongue, reflecting the more predominantly lower-tropospheric structure of the TD disturbances.

Figure 3 shows a regression of 850-hPa vorticity against itself at the base point 7.5°N, 150°E (this and all other regression plots show only the fields at zero time lag). The wavelike structure is similar to that seen in earlier studies. The signal would be slightly stronger and the wavelike nature more apparent if we had chosen a point farther north and west. For example, a plot using the same base point as Fig. 4 of Lau and Lau (1990) (not shown) looks much the same as that figure. Again, though, we wish to focus on the southeastward portion of the TD disturbance storm track.

We have computed the phase speed from the regressed 850-hPa vorticity using the method of LL90, at a number of base points. This method involves tracking the vorticity maximum as a function of time lag. The results are in general agreement with those shown in the upper panel of their Fig. 6, that is, of order 3 m s⁻¹, roughly toward the northwest. If we perform the same calculation in the Atlantic basin, we get typically somewhat larger phase speeds, which is also in agreement with their results.

The fact that every quantity we have computed that is directly comparable to one presented in LL90 is in good agreement with their results suggests that the NCEP–NCAR reanalyses we have used do not have major differences with the ECMWF operational analyses that LL90 used, as far as the disturbances in question are concerned. This generally bolsters our confidence in the usefulness of both datasets.

c. Example case

To communicate a bit more intuitive feeling for the behavior of TD disturbances, we show in Fig. 4 a sequence consisting of 850-hPa unfiltered absolute vorticity contours plotted at 0000 UTC of 10, 15, and 20 August 1994.

Various troughs have been given labels to aid the reader in tracking them. The continuity of each feature from one frame to the next is more obvious when one views the analogous plots from each day in between those shown here, but the wide temporal spacing has been judged necessary here for compactness of presentation, given that phase propagation of these disturbances is quite slow. Here “17,” “18,” and “19” represent Super Typhoons 17, 18, and 19. The last is barely even noticeable as a wave trough in the first frame but

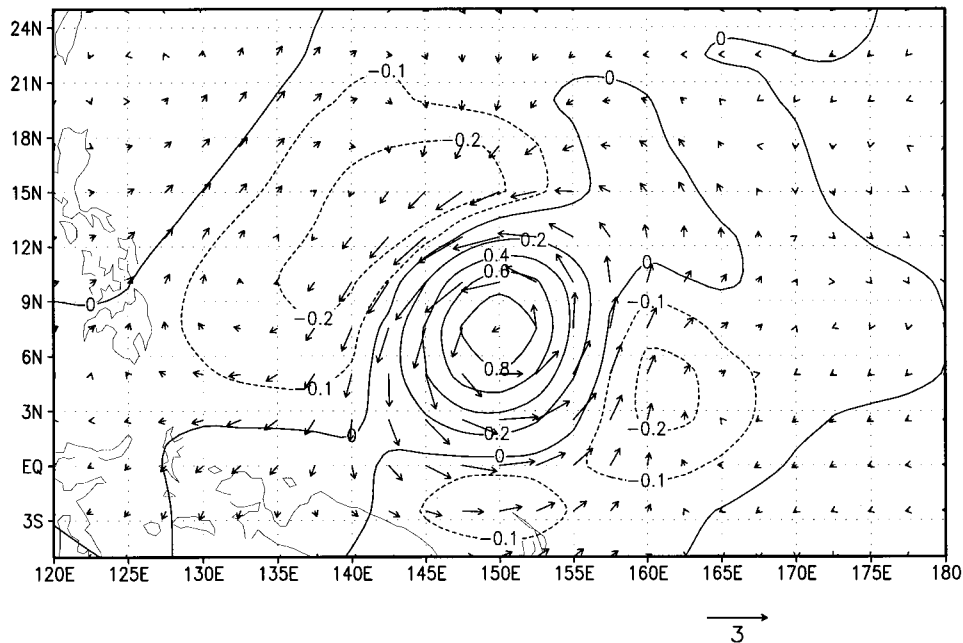


FIG. 3. Bandpassed 850-hPa vorticity regressed against itself at a reference point of 7.5°N, 150°E, and zero time lag (10^{-5} s^{-1}). Note that contour interval for negative values is half that for positive ones. Regressed 850-hPa horizontal wind (m s^{-1}) is also shown.

had reached typhoon strength by the second. Other wave troughs have been labeled with letters “A” through “E.”

The feature of most significance here is the overall compression of the pattern, resulting in a reduction in the zonal scale of the TD disturbances (disturbances that have reached typhoon intensity, unsurprisingly, cease to be noticeably affected by the zonal convergence), and associated amplitude increase. This is associated largely with the convergence in the zonal wind; shading indicates regions of westerlies, giving some indication of this. Notice the tight clustering of troughs B, C, and E in the last frame, and their wide spacing in the first. The distance between B and E is reduced over this 10-day period from roughly 8000 to 3000 km, and at the same time the amplitudes of B, C, and E have increased substantially. Disturbance C had, in fact, reached tropical depression strength by 19 August, and later intensified into Typhoon 20.

d. Propagation dynamics

We have constructed a vorticity equation using the regression technique. We compute explicitly all terms that depend only on the horizontal wind and treat all others as a residual. We do this partly because the horizontal wind is generally the most accurately observed quantity in the Tropics and the least directly controlled by model parameterizations in assimilated datasets. Also, however, the result will to some extent justify this choice.

Our vorticity equation is, then,

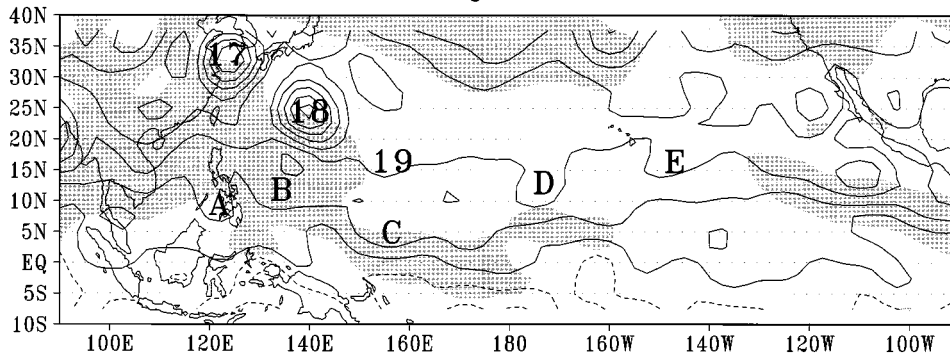
$$\frac{\partial \zeta}{\partial t} + \mathbf{u}_h \cdot \nabla_h \zeta_a = -\zeta_a \nabla_h \cdot \mathbf{u}_h + R, \quad (1)$$

where $\mathbf{u}_h = (u, v)$ is the horizontal wind, ∇_h the horizontal gradient operator, ζ the relative vorticity, and ζ_a the absolute vorticity. The residual R includes vertical advection, vortex-tilting terms, baroclinic generation, and any frictional or subgrid-scale processes. Our procedure is to compute each of the explicit terms directly from each instantaneous data field in the record, time filter the time series of each term at each point, and regress each term separately against the reference time series. If the rhs of (1) were to vanish, the disturbances would obey purely barotropic vorticity dynamics.

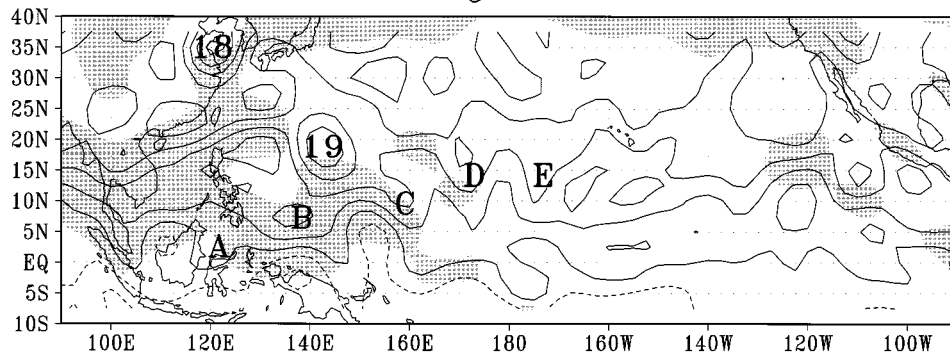
Figure 5 shows patterns of all the explicitly computed terms for the same base point shown in Fig. 3. The tendency and advection terms are almost equal and opposite, suggesting that the propagation is governed mainly by barotropic dynamics. The convergence term is generally smaller than the advection term but, more importantly, maximizes *at* the vorticity maximum, so that it contributes to disturbance growth but almost not at all to propagation. The minimum somewhat north of the trough recurs at many other base points, and so appears to be a real feature, though we do not understand it at present. Also shown is the sum of advection terms from a linearized vorticity equation, that is,

$$v' \frac{\partial \bar{\zeta}_a}{\partial y} + \bar{v} \frac{\partial \zeta'}{\partial y} + u' \frac{\partial \bar{\zeta}_a}{\partial x} + \bar{u} \frac{\partial \zeta'}{\partial x},$$

10 August 1994



15 August 1994



20 August 1994

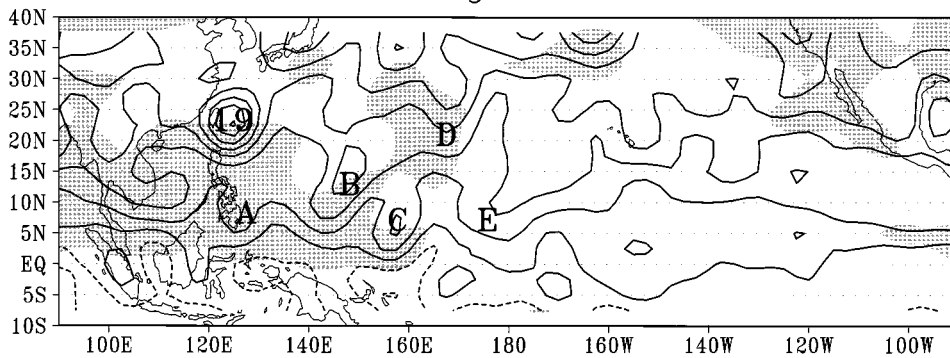


FIG. 4. Sequence of plots of 850-hPa unfiltered absolute vorticity on 10, 15, and 20 August at 0000 UTC. Contour interval is $2 \times 10^{-5} \text{ s}^{-1}$, positive and zero contours are solid lines, and negative contours are dashed. Features labeled as indicated in text. Shading indicates areas of westerly 850-hPa zonal wind component.

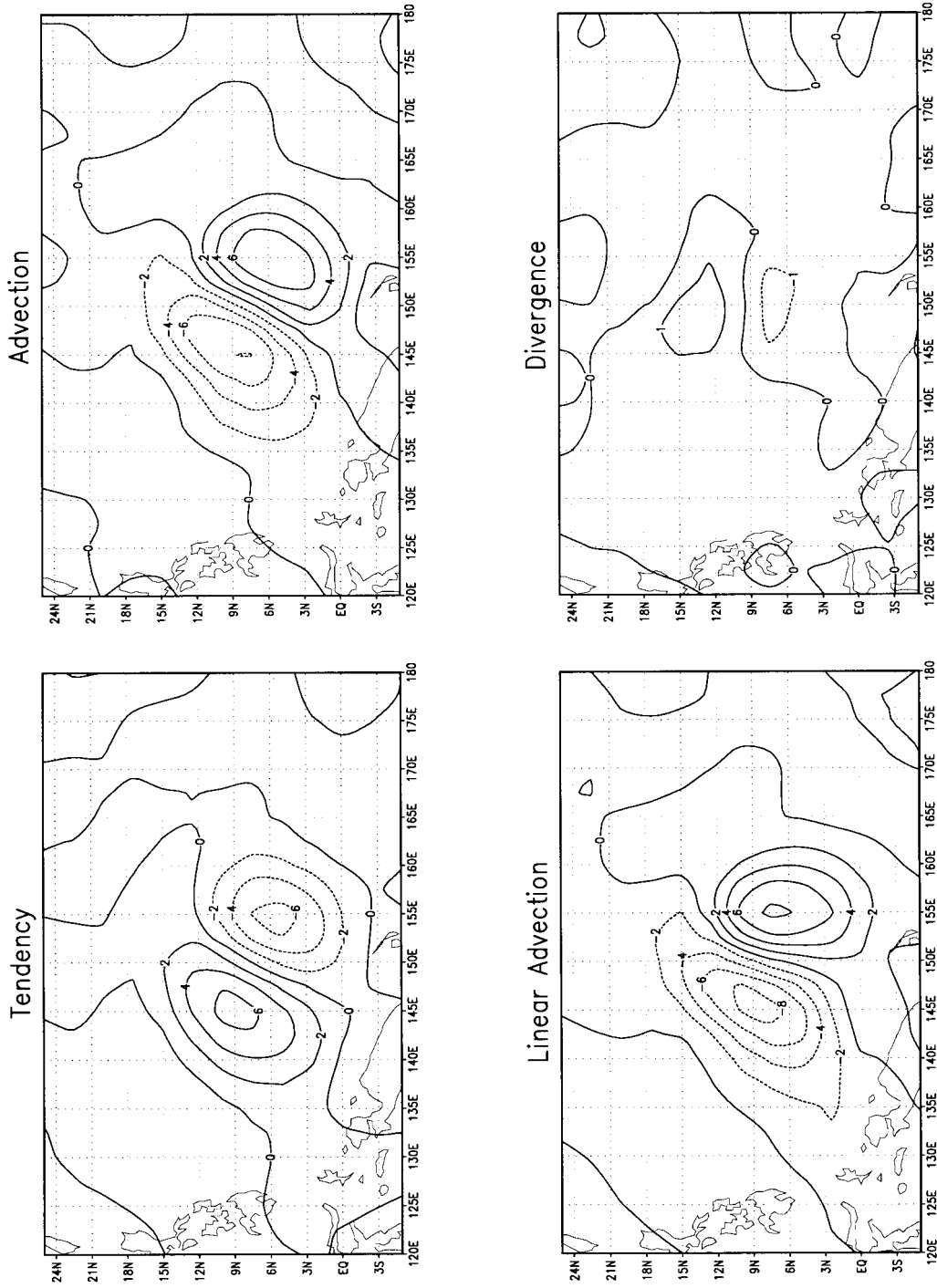


FIG. 5. Explicitly computed terms in the 850-hPa vorticity equation (see text) regressed against vorticity at the same base point as in Fig. 3: (upper left) tendency $\partial\zeta/\partial t$, (upper right) advection $\mathbf{u} \cdot \nabla \zeta$, (lower left) linear advection terms $\bar{\mathbf{u}} \cdot \nabla \zeta' + \mathbf{u}' \cdot \nabla \bar{\zeta}$, (lower right) divergence $\nabla \cdot \mathbf{u}$. Units are 10^{-11} s^{-2} . Note that contour interval for the divergence term is half that used for the others.

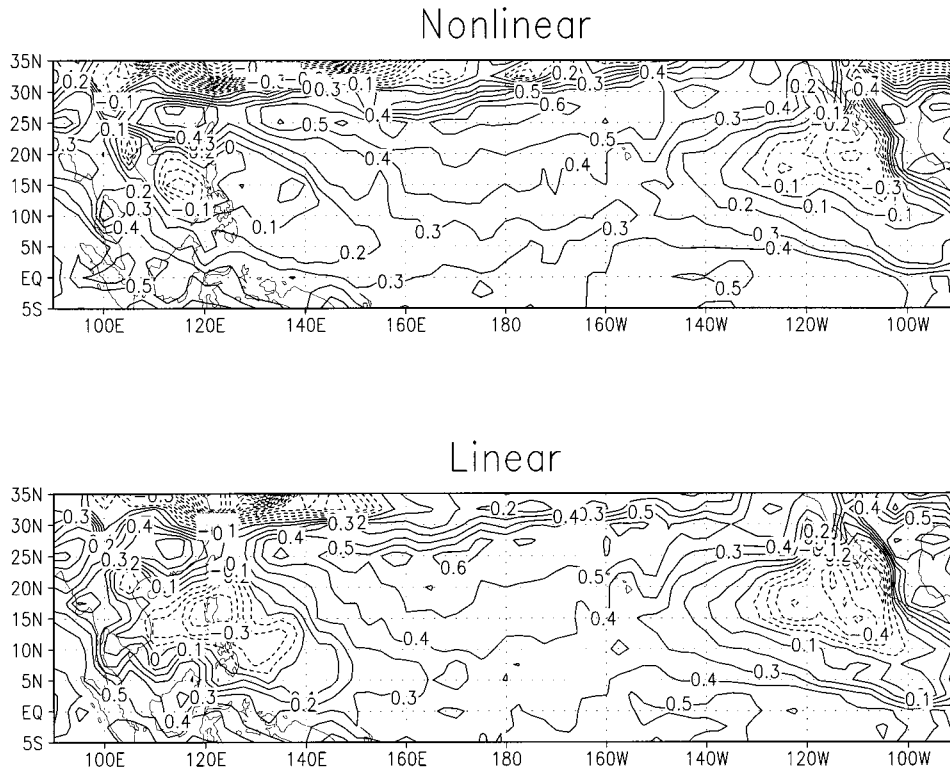


FIG. 6. Fractional difference between observed and barotropic phase speeds (see text). (upper) Calculation uses full nonlinear advection terms; (lower) calculation uses linearized advection terms. In both cases, positive numbers indicate that disturbances travel slower than they would under pure barotropic (either linear or nonlinear) dynamics.

where the overbar refers to a time average over the entire data record and the prime refers to deviations from that average. Note that this gives essentially the same result as the full advection term, indicating that the disturbances at this base point are not only governed by barotropic vorticity dynamics, but by the Rossby wave terms (as opposed to, e.g., advection of a closed vortex by a mean flow on an f plane). This is in agreement with the results of Shapiro (1978), and to a lesser but still significant extent with those of Stevens (1979), for easterly waves in the Atlantic.⁴ Davidson and Hendon (1989) also came to a similar conclusion regarding TD-like disturbances in the southern Pacific. Regarding the WP region specifically, our results are in rough agree-

⁴ We note that Stevens argued, based on his results, that the waves were *not* governed by barotropic vorticity dynamics, in contradiction to Shapiro's (1978) results. However, Stevens's (1979) results only partially support that claim. In his Fig. 1 (middle row, left), the tendency and horizontal advection terms do nearly cancel, within a reasonable inference as to the noise level of the data, over most of the wave phase. Stevens's disagreement was apparently based entirely on his single "bull's-eye" of noncancellation between these terms, centered at about 600 hPa and just downstream of the trough.

ment with those of Lau and Lau (1992) for the region south of the main axis of their composite.

Figure 6 shows the spatial pattern of this behavior, as follows. For each base point, we regress both the tendency term and the horizontal advection term at all other points against the vorticity time series at that point. We then locate the point where the tendency maximizes, as well as the point where the advection minimizes. These two points are generally either the same or very near one another, as in the example in Fig. 5. We then use these maximum and minimum values, respectively, to compute the fractional difference between the observed phase speed and the phase speed that would be observed if the waves were governed purely by horizontal vorticity advection and nothing else. That is, for a propagating, sinusoidal wave, with amplitude constant in time, the phase speed would be equal to

$$c_p = \frac{\left(\frac{\partial \zeta}{\partial t}\right)_{\max}}{k \zeta_{\max}}, \quad (2)$$

where $(\partial \zeta / \partial t)_{\max}$ is the maximum value of the tendency

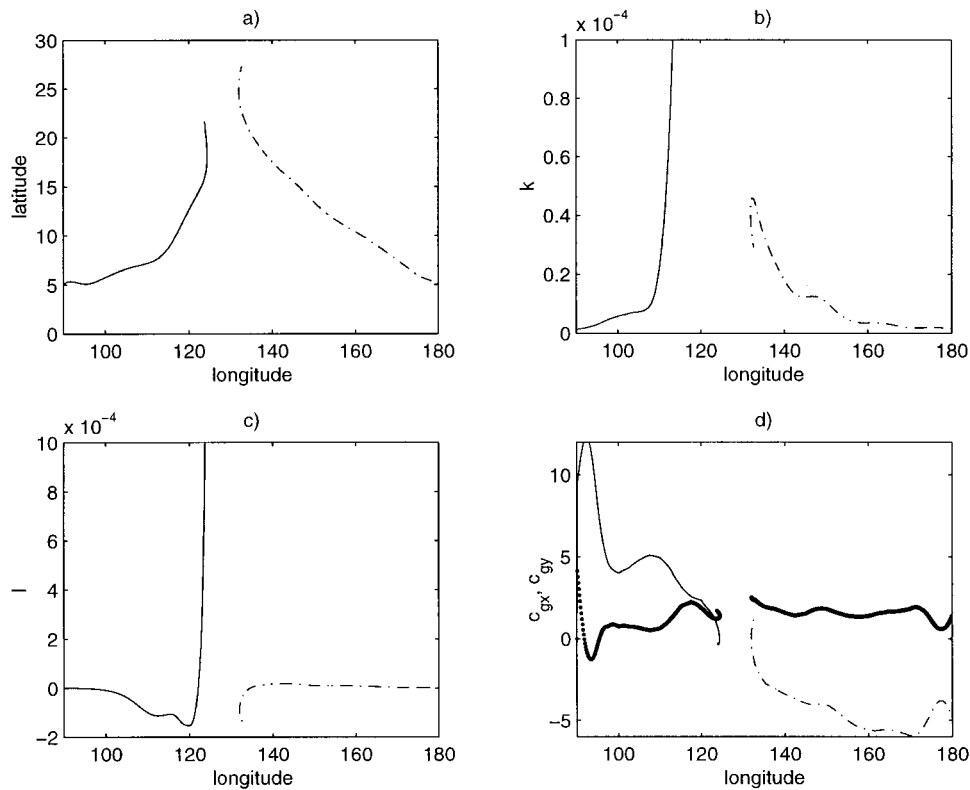


FIG. 7. Results of two ray-tracing calculations. One (solid) begins at 5°N, 180°, with zonal and meridional wavenumbers both corresponding to wavelengths of 4000 km; while the other (dot-dash) starts at 5°N, 90°E, with zonal and meridional wave numbers both corresponding to wavelengths of 5000 km. (a) Wave packet longitude, (b) zonal wavenumber k (m⁻¹), (c) meridional wavenumber l (m⁻¹), (d) zonal (light) and meridional (heavy) group velocities (m s⁻¹). Each meridional group velocity curve belongs to the calculation whose zonal group velocity curve (distinguishable by solid vs dot-dash) occupies the same longitude range.

(located one quarter-wavelength ahead of the vorticity maximum); ζ_{\max} is the value of the vorticity maximum; and k is the horizontal wavenumber, evaluated along a coordinate axis parallel to the direction of propagation. For a pure barotropic, inviscid Rossby wave, we would have

$$\left(\frac{\partial \zeta}{\partial t}\right)_{\max} = -(\mathbf{u}_h \cdot \nabla_h \zeta_a)_{\max};$$

hence, we estimate the fractional difference from pure barotropic, inviscid behavior by the quantity

$$\frac{\left(\frac{\partial \zeta}{\partial t}\right)_{\max} + (\mathbf{u}_h \cdot \nabla_h \zeta_a)_{\max}}{(\mathbf{u}_h \cdot \nabla_h \zeta_a)_{\max}}. \quad (3)$$

This is, strictly, the fractional difference in the maximum tendency, but since the only other quantity appearing in (2) is the wavenumber k , which we may take as a fixed constant, this is equivalent to a fractional difference between the observed phase speed and the hypothetical barotropic inviscid one.

It should be noted that, for a wave experiencing

growth or decay as well as propagation, the maximum value of the tendency includes information about the growth or decay as well, and so Eq. (2) is not strictly valid. However, it is easily shown that the relative error associated with the neglected term in that expression scales as τ_p/τ_g , where τ_g is the time over which the amplitude doubles, and τ_p is the time over which the wave propagates a distance of a quarter-wavelength, $\lambda/4c_p$, with λ being the wavelength. Taking the wavelength to be roughly 2000 km and the phase speed to be 3 m s⁻¹, this time is roughly 1.5 days. The growth time may be estimated by dividing the typical growth rate computed by LL90, shown in the upper panel of their Fig. 7, by the typical magnitude as expressed by the vorticity variance. The former has a magnitude $\sim 10^{-6}$ s⁻¹ day⁻¹, while the latter is around 10^{-5} s⁻¹, yielding a growth time of around 10 days, so that the tendency maximum can be assumed to be dominated by propagation. Note that a 10-day growth rate, and the observed phase speeds, implies that a typical wave doubles in amplitude while propagating over a distance comparable to the size of the entire region over which the disturbances are observed. Since LL90's calculations presumably include cases of tropical cyclogenesis in-

volving significantly faster growth over certain periods, we may reasonably infer that noncyclogenetic disturbances may in some cases experience substantial periods of zero growth, or even decay.

Figure 6 shows the quantity in Eq. (3), evaluated at every base point and plotted as a contour map. Note that positive numbers indicate disturbances that travel more slowly than they would under pure barotropic dynamics. The upper panel shows the calculation done using the full nonlinear advection terms, while the lower panel shows that using linearized advection. Along the southeastward portion of the TD storm track, the 850-hPa disturbances propagate with phase speeds around 20%–30% slower than they would if governed by barotropic, inviscid, linear vorticity dynamics. There is little difference between the linear and nonlinear calculations in this southeastward portion of the storm track, indicating that the small, but persistent and spatially coherent, difference from the linear advection speed is not due to nonlinearity. Given some uncertainty in the observational analyses, and the fact that it is not usually possible to rigorously justify the application of very simple conceptual models to tropical disturbances (unlike in midlatitudes, e.g., where quasigeostrophy is generally believed to give at least a qualitatively good description of many important phenomena), this calculation provides relatively solid justification for the assertion that the disturbances propagate approximately as layerwise barotropic, inviscid Rossby waves at 850 hPa, in their earlier stages of development. This is despite the fact that they are closely associated with deep convection, violating the key assumption of Charney's (1963) scale analysis.

This is not a totally new result, since Shapiro (1978) and Stevens (1979) showed it to be true for Atlantic easterly waves, Davidson and Hendon (1989) showed it for southern Pacific TD-like disturbances, and LL92 provided evidence that it was to some extent also true in the WP. Nonetheless, our analysis brings this result to the fore and provides (to our knowledge) the second confirmation of this result for the western Pacific region.⁵

In the more northwestward portion of the storm track, near the Philippines, the agreement between the nonlinear advective and observed phase speeds improves, while that between the linear and observed ones changes sign and becomes larger in magnitude. It is plausible to associate the increasing difference between the linear and nonlinear calculations with the development of

more strongly nonlinear disturbances, that is, tropical cyclones. This does not, however, explain the fact that the nonlinear advective tendency agrees better with the observed one in the northwestward than the southeastward region. This may perhaps be an artifact of viewing structures (i.e., tropical cyclones), which feel the mean winds over a deep layer in terms of advection at a single level. Both the prevalence of tropical cyclones and the typical vertical shear are larger in the northwestward than the southeastward region.

4. Ray tracing

Given that the disturbances propagate according to a simple and well-understood theoretical model (the barotropic, inviscid Rossby wave), a number of theoretical tools are available for further analysis of their expected behavior. Possibly the simplest of these is classical ray tracing, as in Lighthill (1978).

This technique represents a hypothetical wave packet containing a spread of wave numbers centered on some initial assumed value, implying initial values for phase and group velocities through the dispersion relation, and centered physically at some given initial point. The wave packet is thus represented explicitly only as a single point in both physical and wavenumber space. The trajectory of the wave packet in physical space is fully determined by the instantaneous group velocity. In two dimensions, this is expressed as

$$\begin{aligned}\frac{dx}{dt} &= c_{gx} = \bar{u} + \frac{\partial \omega}{\partial k} \\ \frac{dy}{dt} &= c_{gy} = \bar{v} + \frac{\partial \omega}{\partial l},\end{aligned}$$

with (x, y) representing zonal and meridional position, c_{gx} and c_{gy} zonal and meridional group velocity, ω the frequency perceived by an observer moving with the mean flow (\bar{u}, \bar{v}) , and k and l zonal and meridional wavenumbers. As the packet propagates, its wavenumbers change according to the relations

$$\begin{aligned}\frac{dk}{dt} &= -k \frac{d\bar{u}}{dx} - l \frac{d\bar{v}}{dx} - \frac{\partial \omega}{\partial x} \\ \frac{dl}{dt} &= -l \frac{d\bar{v}}{dy} - k \frac{d\bar{u}}{dy} - \frac{\partial \omega}{\partial x}.\end{aligned}$$

The last term on the rhs in both expressions is due to variations in the dispersion relation as a function of space due to properties of the mean state (e.g., variations in vorticity gradients, for Rossby waves).

Ray tracing is only strictly valid when the waves obey a WKB assumption. That is, that the mean flow must vary slowly compared to the wavelength. This assumption is certainly violated to some extent by the flow shown in Fig. 1, assuming a wavelength of at least 2000 km. Nonetheless, WKB theory is in many problems

⁵ We add that Reed and Johnson (1974) performed a vorticity budget analysis of the Reed and Recker (1971) composites, which in principle could have also shed light on this question. However, Reed and Johnson only presented calculations of the advection and tendency terms precisely in the trough, where both approximately vanish essentially by definition; hence, their results cannot be used to derive any information about the propagation dynamics.

found to give qualitatively correct results even when the slowly varying assumption is fairly strongly violated. We use it with this in mind.

We have performed a number of ray-tracing calculations using the climatological 850-hPa mean flow shown in Fig. 1, and using the dispersion relation for linear, barotropic, inviscid Rossby waves:

$$\omega = \frac{-\frac{\partial \bar{\zeta}_a}{\partial y} k}{k^2 + l^2}.$$

Similar calculations have been performed in a study of Atlantic easterly waves by Skubis et al. (1997).

Figure 7 shows two representative examples from our calculations. One starts from an initial position of (5°N, 180°) with zonal and meridional wavelengths both equal to 4000 km, while the other starts from (5°N, 90°E) with wavelengths of 5000 km. The wavelengths are chosen simply to be somewhat larger than a typical TD disturbance, since wave accumulation causes a reduction in wavelength. In both cases, the packet initially propagates toward the monsoon trough region (i.e., the first goes westward, while the second goes eastward). As they approach this region, both packets experience decreases in group velocity toward very small values, and increases in k and l toward values that are essentially infinite, at least in the sense that the linearization will have broken down long before these values are achieved. Farrell and Watterson (1985) provide a more sophisticated and thorough analysis of linear theory's predictions in situations such as this. For our purpose the main point is that we expect Rossby waves to experience some decrease in wavelength, and increase in amplitude, before nonlinearity becomes important. While wave energy is not conserved, due to the forced nature of the mean flow (as indicated by the flow across vorticity contours in Fig. 1), a wave activity that is closely related (in some cases identical) to wave enstrophy is conserved, if the mean vorticity contours are approximately zonal (Young and Rhines 1980; Plumb 1986), which Fig. 1 shows that they are (at 850 and 500 hPa). The intrinsic group and phase speeds of short (relative to the planetary scale) Rossby waves are both very small, $O(1 \text{ m s}^{-1})$, so the group velocity is to a first approximation simply equal to the mean flow velocity. The convergence of wave activity is, then, determined approximately by the horizontal convergence of the mean flow. Because the mean flow convergence is dominant, the results presented in this section are quite insensitive to the wavenumbers chosen, including the direction in which the wave tilts, as long as k and l are not both very small. We have verified this by a number of calculations using many values of k and l , including $l = 0$ (as long as k is not also zero or very small in that case).

5. Wave activity diagnostic

Plumb (1986) developed a three-dimensional wave activity flux for small-amplitude, quasigeostrophic eddies on a slowly varying time-mean flow. This flux is computed from eddy statistics, and hence provides information that is fundamentally different, and partly independent, from that provided by techniques that depend only on the mean flow (such as ray tracing). Since the Coriolis parameter is small in the region of interest here, it is inappropriate to regard the disturbances as quasigeostrophic. However, the "Plumb flux" is valid for two-dimensional barotropic disturbances on a two-dimensional mean flow, whether quasigeostrophic or not, because these satisfy a vorticity conservation law. In this case, the relevant wave activity is obtained simply by neglecting all baroclinic terms in Plumb's Eq. (2.20), the result being that the wave activity is defined as

$$M = \frac{p \overline{\zeta'^2} \cos \phi}{|\nabla \bar{\zeta}_a|}, \quad (4)$$

with ϕ the latitude and p the pressure. The barotropic version of the Plumb flux then has a radiative part [see Plumb's Eq. (2.23)],

$$\mathbf{M}_R = p \cos \phi \left[\frac{1}{2} (\overline{v'^2} - \overline{u'^2}), -\overline{u'v'} \right],$$

where again the mean vorticity contours have been assumed zonal; and an advective part, so that M satisfies the conservation relation

$$\frac{\partial M}{\partial t} + \nabla \cdot (\mathbf{M}_R + \bar{\mathbf{u}}M) = S_M.$$

Here S_M is a source term related to nonconservative sources and sinks of eddy vorticity, and $\bar{\mathbf{u}} = \bar{\mathbf{u}}_h$. The Plumb flux satisfies the group velocity property, so that in the "almost-plane wave limit," the group velocity is

$$\mathbf{c}_g = \frac{\mathbf{M}_R + \bar{\mathbf{u}}M}{M}. \quad (5)$$

Application of the Plumb flux, like ray tracing, requires assumptions that the waves are linear and the flow is slowly varying. Again, we use this diagnostic despite the partial violation of these assumptions (particularly the latter), with the expectation that it still provides useful information.

We have computed the barotropic Plumb flux and wave activity from the 850-hPa wind and vorticity data, all time filtered as in the previous section, and used these to compute the group velocity according to (5). The upper panel of Fig. 8 shows M_R/M , the radiative part of the group velocity, and contours of its divergence where it is less than $-1 \times 10^{-6} \text{ s}^{-1}$. Note that in some parts of the TD storm track the zonal component is slightly westward, which might seem to contradict our

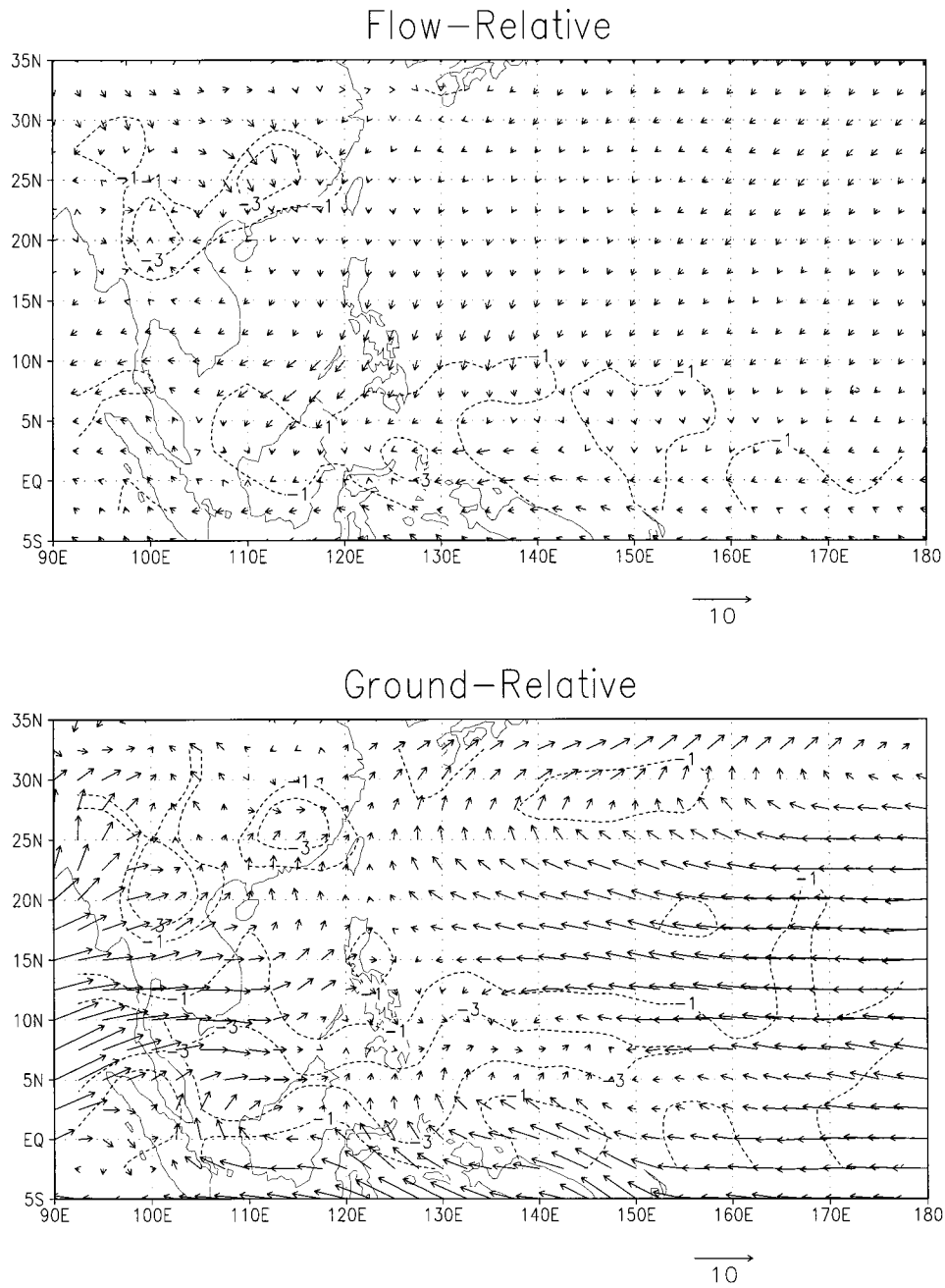


FIG. 8. (upper) Radiative, i.e., flow-relative, part of the group velocity, calculated from bandpassed velocity and vorticity fields using the barotropic Plumb flux (m s^{-1}) and its divergence (10^{-6} s^{-1} ; only negative contours plotted). See text for details. (lower) As in upper panel but for the total ground-relative group velocity, which is the flow-relative part shown in the upper panel plus the mean flow velocity.

claim that the disturbances propagate as Rossby waves, given their synoptic-scale wavelengths (since these imply eastward phase speeds). However, this component is very small and depends on the difference between $\overline{v'^2}$ and $\overline{u'^2}$, which have distributions (not shown) very similar to one another, so that this component is a small difference of large numbers. Therefore, we do not consider this inconsistency a serious problem, given some

degree of uncertainty in the data; the main point is that the zonal component is in any case small. The meridional component is somewhat larger and persistently southward in the region of interest.

The lower panel of Fig. 8 shows the total (i.e., ground relative) group velocity, as well as its divergence (again where it is less than the same threshold value as above). Note the large area of significant convergence in a re-

gion collocated with substantial TD wave activity. This convergence exceeds $3 \times 10^{-6} \text{ s}^{-1}$ over a region whose length is similar to a TD wavelength in the longitudinal dimension (though significantly narrower meridionally), and somewhat smaller, though still significant values over a larger region. The convergence of the group velocity tells us the rate at which wave activity accumulates and, having units of inverse time, is thus a direct estimate of the local "growth rate" one expects by this mechanism. Here $3 \times 10^{-6} \text{ s}^{-1}$ corresponds to a growth timescale of roughly 3 days; $1 \times 10^{-6} \text{ s}^{-1}$ corresponds roughly to 10 days. As expected, this convergence of the group velocity is dominated by the convergence of the mean flow, that is, $|\mathbf{M}_R| \ll |\mathbf{uM}|$. However, we note that the convergence of the flow-relative group velocity does make a noticeable, if secondary, contribution to that of the ground-based group velocity. In the EP region the 850-hPa group velocity convergence (not shown) does not exceed $1 \times 10^{-6} \text{ s}^{-1}$ over an appreciable area, again illustrating that the dynamics of WP and EP disturbances may well be different, at least as far as their initial growth is concerned.

LL92 computed enstrophy dissipation timescales of a few days in the northwestward part of the WP storm track from their composites. It is plausible that the actual dissipation timescale for noncyclogenetic or precyclogenetic disturbances is a bit longer, given some tropical cyclone contamination of the LL92 composites (one expects tropical cyclones to feel strong dissipation due to their large surface wind speeds, leading to increased surface drag coefficients). Hence, the wave activity convergence appears at least competitive with the best current estimate of the dissipation rate which TD disturbances experience.

It should be stated that our entire argument is consistent only in the band centered around 5° – 10° N, and spanning longitudes between 130° and 170° E. Only there is the phase propagation most nearly indicative of linear, barotropic dynamics, the group velocity convergence significant, and the actual wave amplification observed. This is, however, the actual beginning portion of the TD storm track, and hence the region of most interest. There is a band of equally large group velocity convergence centered closer to the equator and between longitudes 100° and 130° E where wave amplification is not observed, on average (as evidenced by Fig. 2). It seems likely that this is attributable to the larger vertical shear in this region. To substantiate this, Fig. 9 shows the zonal and meridional components of the total tropospheric shear, defined as the wind at 200 hPa minus that at 850 hPa, computed from the time-mean fields shown in Fig. 1. The TD storm track corresponds roughly with a local minimum in the absolute value of this shear.

6. Correlation between mean westerlies and disturbance enstrophy

The monsoon westerlies are a key ingredient in the wave activity convergence. To illustrate this, we show

in Fig. 10 three time series, computed as follows. First, we divide our entire data record into 10-day periods (throwing away the few odd days that remain, since the period 15 May–15 September is not evenly divisible by 10 days). For each 10-day period, we compute the standard deviation of time-filtered vorticity, and the integrated zonal divergence in a box spanning 5° – 15° N and 150° – 170° E [note that this includes the "KEP" triad of stations studied by Reed and Recker (1971)]. Then, we compute the average zonal wind over a box displaced 10° W, that is, 5° – 15° N and 140° – 160° E. This displacement is chosen since it is the wind flowing into the region of interest, rather than through it, that is expected to be most important. These three curves are shown in Fig. 10. The standard deviation of vorticity is given in units of its average value over the record ($7.5 \times 10^{-6} \text{ s}^{-1}$), while the other two curves are normalized by their standard deviations, and the mean is subtracted from each resulting time series. The (record) mean and standard deviation of the zonal wind are -2.5 and 3.0 m s^{-1} , respectively, while those of the integrated zonal divergence (which is simply the zonal wind at the eastern boundary minus that at the western boundary) are -2.9 and 1.9 m s^{-1} .

The correlation coefficient between the zonal divergence and vorticity variance is -0.58 , while that between the vorticity variance and the offset zonal wind is 0.73 , illustrating the importance of the rather special climatological situation in the WP region resulting from the eastward protrusion of the lower-level monsoon westerlies. Interestingly, the prominent role of the westerlies in the WP region was also noted by Riehl (1948).

7. Sources of wave activity

The wave accumulation mechanism assumes that there is some degree of Rossby wave activity outside the WP region, at wavelengths longer than that of the TD disturbances. The sources of this wave activity will not be conclusively identified here. Some reasonable speculations may be made, however.

It is possible that westward group propagation and convergence of the MRG mode could result in development of TD disturbances. The group velocity analyses done in this paper do not shed any light directly on this, as the MRG mode is not barotropic. However, it is quite suggestive that the MRG mode is most clearly observed in the central Pacific and has a longer wavelength than the TD mode. If a lower-tropospheric, central Pacific MRG wave packet were to experience westward group propagation, combined with zonal convergence, linear theory would predict that its wavelength would shorten, its amplitude would increase, and its structure would become more Rossby-like, providing a clear explanation for the change from MRG- to TD-type behavior that is observed from the central Pacific to the WP region. One also would have to explain the breaking of the neat antisymmetry about the equator associated with the

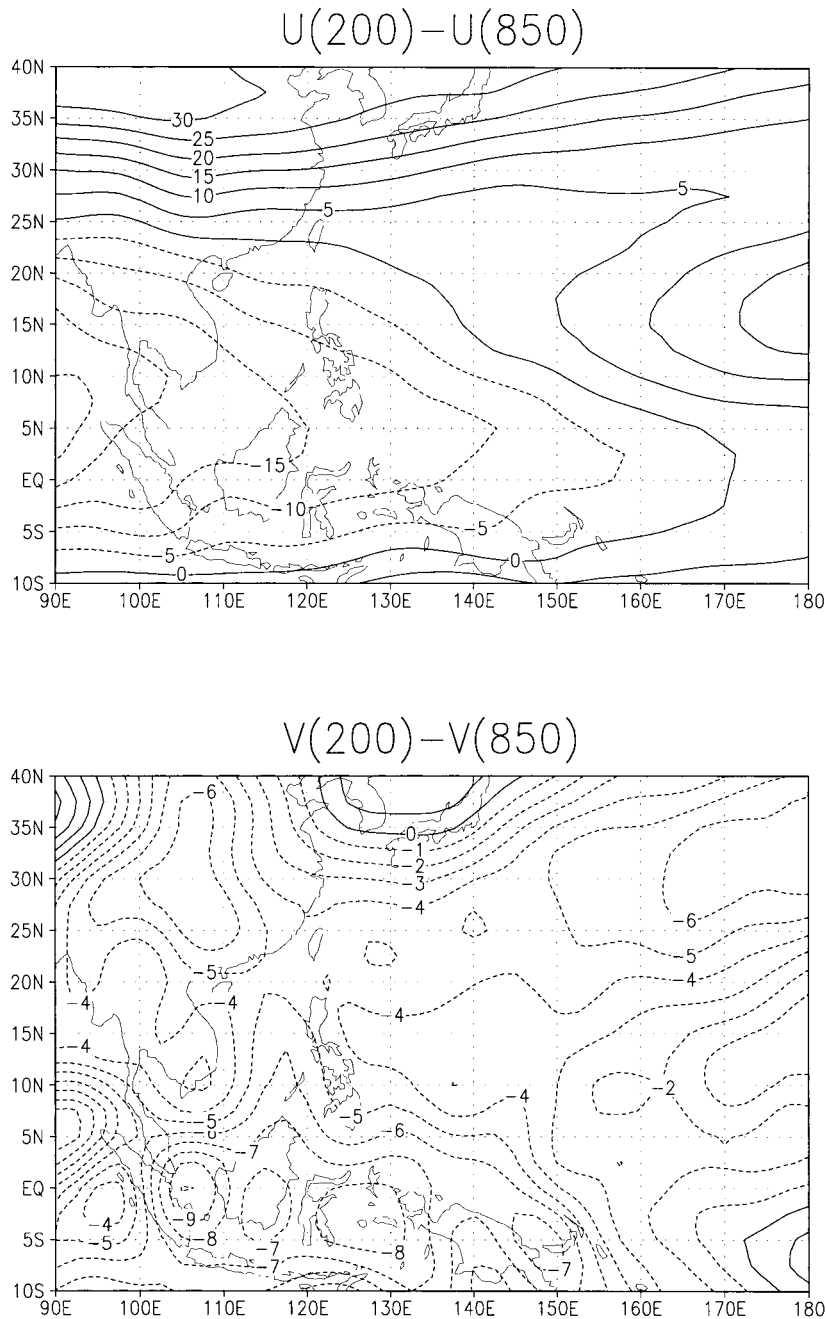


FIG. 9. (upper) Time-mean zonal wind at 200 hPa minus that at 850 hPa (m s^{-1}); (lower) as in upper panel but for meridional wind.

MRG mode, to produce the one-sided off-equatorial structure of the TD mode. This might well be associated with the complex structure of the time-mean wind field at lower levels, something not allowed in the analytically solvable linear models typically used to explain the dispersion characteristics of equatorial waves.

The weakest link in this hypothesis at present is the ambiguity in the group velocity of the MRG mode. The

intrinsic (flow relative) group velocity is eastward according to linear theory, but the magnitude depends on the wavelength and the equivalent depth chosen. Generally one expects magnitudes in the range $5\text{--}10 \text{ m s}^{-1}$, which is comparable to the easterly low-level mean flow in the central Pacific, leaving the ground-relative group velocity ambiguous. Liebmann and Hendon (1990) estimated MRG group velocities observationally and ob-

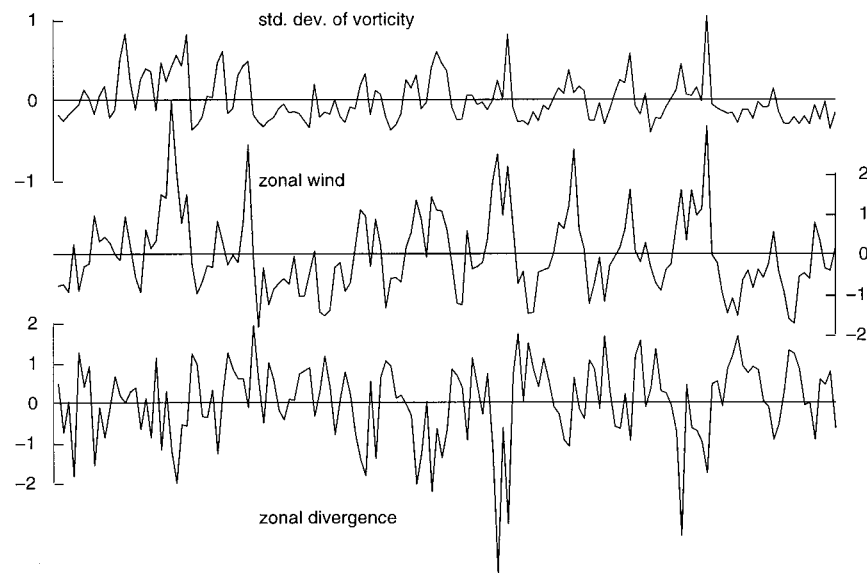


FIG. 10. Time series of standard deviation of bandpassed vorticity (upper curve), integrated zonal divergence (lower curve, with \times 's), and zonal wind (middle curve, dot-dash), averaged over 10-day periods and $20^\circ \times 10^\circ$ areas. The abscissa spans the entire data record. Zonal wind is computed in a box displaced westward by 10° longitude from the others. The standard deviation of vorticity is normalized by its mean value, while the zonal wind and divergence are normalized by their standard deviations, and the mean of each series is then removed.

tained values that were generally positive (eastward), but quite close to zero in the central Pacific, for the September–December season. Dunkerton and Baldwin (1995) performed a similar analysis for a data record spanning 10 entire years, but did not present results explicitly pertaining to the zonal component of the group velocity in the lower troposphere in northern summer. The possibility that MRG waves may “seed” TD disturbances has been raised by Takayabu and Nitta (1993) and Dunkerton and Baldwin (1995), though without mentioning the convergence mechanism.

In addition to acting upon wave activity generated by any external source, the strong convergence in the WP will act to prevent any Rossby waves generated in situ from leaving the WP region. We expect that mature tropical cyclones will be an important source of these waves.

Generally, one expects that a strong monopolar vortex in the vicinity of a vorticity (or PV) gradient will excite Rossby waves (e.g., Flierl et al. 1983; McWilliams et al. 1986). Specifically, the excitation of waves by tropical cyclones has been discussed by Davidson and Hendon (1989), Holland (1995), and Ferreira and Schubert (1997). Figure 11 shows daily averaged vorticity and wind fields at 850 hPa on 26 June 1997. Note the similarity to Fig. 12 of Holland (1995) or Fig. 7 of Ferreira and Schubert (1997), which show results of model experiments intended to illustrate this process. The typhoon circulation deforms the absolute vorticity contours to its southeast strongly northward, inducing an anticyclonic circulation there, which in turn induces a

second trough to its own east. This is Rossby wave propagation. Incidentally, some physical understanding of the southward meridional component of the flow-relative group velocity that was evident in Fig. 8 can be gained from this figure.

Situations of this type are more nearly the rule than the exception during the summer season in the WP region, as represented by the NCEP–NCAR reanalyses. The climatological average number of mature tropical cyclones that occur in the WP is around 27 (Gray 1979). Given that most of these occur between, say, May and December, and that the typical lifetime of a mature tropical cyclone is on the order of a week, to a reasonable zeroth approximation, there usually is one somewhere in the region during the summer.

Therefore, we expect that mature tropical cyclones are a *climatologically important* source of TD disturbances, some of which then develop into tropical cyclones themselves. This suggests an explanation for the observed wavelength of at least some TD disturbances, since one expects tropical cyclones to excite waves most strongly at the spatial scale of the synoptic-scale circulation associated with the cyclone. In this case, the wave accumulation mechanism functions in a secondary but complementary way to that of tropical cyclone wave radiation, by preventing the waves thus generated from escaping or dispersing.

8. Conclusions and discussion

We have argued that wave accumulation is an important mechanism in the development of TD distur-

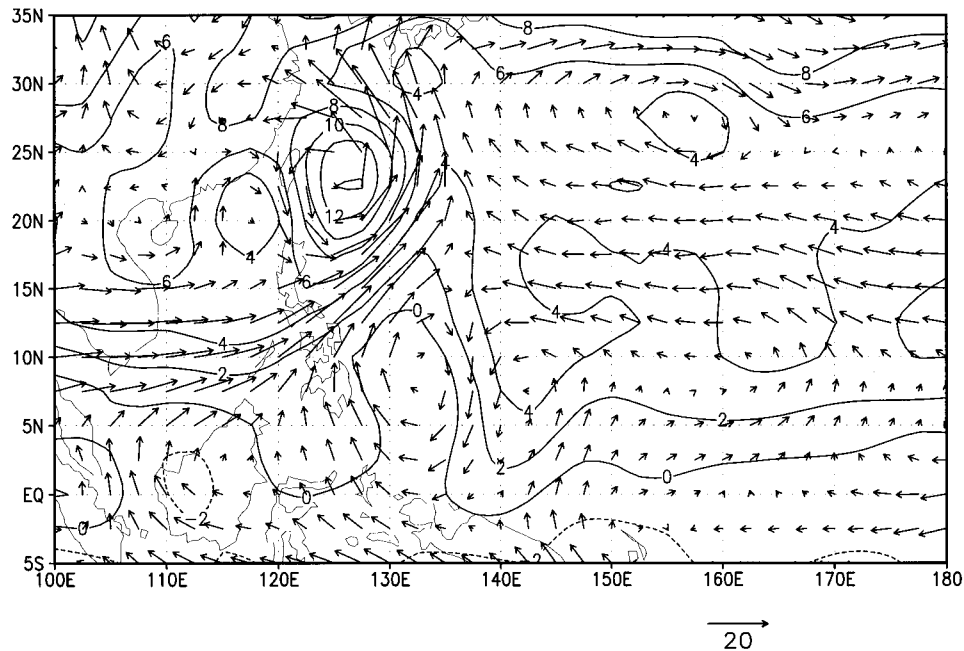


FIG. 11. The 24-h averaged 850-hPa vorticity (10^{-5} s^{-1}) and wind fields (m s^{-1}) from 26 Jun 1997. The large vorticity maximum is Typhoon Peter.

bances in the WP region. The first point of our argument is that TD disturbances propagate essentially as barotropic Rossby waves on the lower-level flow. This fact justifies the use of analysis tools such as ray tracing and the barotropic version of the Plumb flux. Both of these support the second and main point of our argument, that wave accumulation occurs strongly in the WP. The Plumb flux calculation leads to an estimate of the local growth rate (simply equal to the convergence of the group velocity), which at its large-scale maximum reaches 0.3 day^{-1} , a value large enough that this mechanism must be taken seriously. We have also argued that mature tropical cyclones are likely to be a climatologically important source of waves, and that the wave accumulation mechanism acts in concert to prevent the dispersion of the waves thus generated.

The assumptions sufficient to guarantee conservation of the wave activity used here are not sufficient to guarantee conservation of wave energy. A barotropic conversion term is present in the budget for the latter but not the former [for relevant discussions of energetics, see Young and Rhines (1980), Hoskins et al. (1983), and Farrell and Watterson (1985)]. Hence, the wave convergence mechanism discussed here can in general be perfectly consistent with the idea that barotropic conversion of mean to eddy kinetic energy is important in the disturbance energetics, as suggested by LL92, as long as the conversion is nonmodal. This conversion will be invisible from the point of view of Plumb's wave activity. In a flow that allows barotropically unstable normal modes, the mean vorticity gradient must change

sign, in which case the definition of Plumb's wave activity breaks down. This situation was not encountered here. In any case, however, it should be kept in mind that despite their apparently barotropic propagation at 850 hPa, the TD disturbances are not *energetically* barotropic (Nitta 1970, 1972; Reed and Recker 1971; LL92).

A great deal has been left unanswered. Particularly important is the question of how the convection and synoptic-scale flow interact. While we have not addressed this issue directly, the present results do have some implications that are relevant to it.

As mentioned in the introduction, a number of studies have taken the correlations between heating, vertical velocity, and temperature to imply that TD disturbances are convectively driven. We have argued here that an entirely independent mechanism is important in their generation. Yet, if a certain amount of speculation concerning matters essentially unknown at present is allowed, our argument may be viewed as consistent with the existing observational evidence.

In the first place, as discussed above, some studies may have overemphasized the role of diabatic heating in the amplification of TD disturbances, as opposed to tropical cyclones, due to the difficulty of separating these two types of disturbances in a completely objective, automated way, particularly when one focuses on the northwestward end of the TD disturbance storm track, by which point most disturbances that are ever going to undergo cyclogenesis have done so. We add that this problem is not totally absent in the present

study either, though we have made some effort to mitigate it (also, we have not addressed disturbance energetics directly in this study in any case).

Second, the wave activity convergence appears primarily limited to a layer perhaps one to at most a few hundred hPa thick in the lower troposphere. Yet TD disturbances are often observed to be considerably deeper than this. It is possible that the disturbance energy generated by diabatic heating is involved primarily in the deepening of the disturbances, leading to an increase in vertically integrated amplitude, without necessarily being responsible for a comparable amplitude increase at low levels. In this regard, it is worth noting that the strongest positive correlations between heating and temperature are typically diagnosed in the upper troposphere.

Third, it is possible that wave activity convergence provides the initiation mechanism for the disturbance, but then that some form of positive convective feedback is activated when the disturbance has reached finite amplitude. Indeed, mature tropical cyclones are the only observed phenomenon for which there is broad agreement on the sign of the feedback between diabatic processes and the large-scale dynamics; it is clearly positive. However, this feedback is known to become operative only when some preexisting disturbance has reached some critical amplitude (e.g., Emanuel 1991, and references therein).

Zehr (1992) has done a comprehensive study of all cases of tropical cyclogenesis and some cases of "non-genesis" (i.e., when a disturbance that appeared potentially cyclogenetic did not become so) in the WP region for two entire years. His findings indicate that genesis is better described as occurring through discrete, rapid transitions than through a slow, steady increase in intensity, and that a typical TD disturbance may in some cases undergo two such transitions before being unambiguously classifiable as a tropical cyclone. Hence, it seems warranted to speculate that the life cycle of a typical TD disturbance could involve an initial growth phase due to wave activity convergence, followed by a first transition in its dynamical character (from being neutral or even damped by feedbacks involving diabatic processes to experiencing a positive such feedback) after finite amplitude is reached, and then in some cases undergoing the second transition (to a true tropical cyclone), but in other cases not. In broad outline, this resembles the three-stage model of tropical cyclone formation proposed by Yanai (1964). Detailed consideration of this hypothesis must almost surely take into account the dynamics of the mesoscale convective systems (or "cloud clusters") into which the convection associated with TD disturbances is often organized, and that appear to be key players in the cyclogenesis problem (e.g., McBride and Zehr 1981; Raymond and Jiang 1990; Zehr 1992; Holland 1995; Ritchie and Holland 1997).

In any case, the main point we wish to make is that

wave activity convergence provides a mechanism for initially weak disturbances to amplify to some extent, independently of any diabatic process (except, of course, that which presumably drives the convergence in the *mean* flow). This does not at all rule out the possibility that some form of convective feedback is important in maintaining the disturbances once they reach finite amplitude, as suggested by a number of observational studies. Rather, it indicates that no *linear* instability mechanism that involves any sort of convective feedback, whether CISK, WISHE, or something else, is necessarily required in order to explain the initial growth of TD disturbances.

In addition to these unresolved issues related to diabatic processes, we repeat that the wave activity convergence mechanism does not by itself explain other important properties of TD disturbances, in particular their observed wavelength, though the mechanism of wave radiation from tropical cyclones may provide a partial explanation for this.

Acknowledgments. We thank K. A. Emanuel, C. P. Guard, R. A. Houze Jr., N.-C. Lau, R. S. Lindzen, J. C. McWilliams, J. D. Neelin, R. A. Plumb, R. J. Reed, J. M. Wallace, M. Wheeler, and M. Yanai for discussions on this work and related subjects, and J. Molinari and two anonymous reviewers for their constructive reviews. AHS is supported by the NOAA Postdoctoral Program in Climate and Global Change, administered by the University Corporation for Atmospheric Research's Visiting Scientist Program. CSB acknowledges support from NASA Grant NAGW-2633 and NOAA under Cooperative Agreement NA37RJ0198.

REFERENCES

- Blackmon, M. L., Y.-H. Lee, and J. M. Wallace, 1984a: Horizontal structure of 500-mb height fluctuations with long, intermediate, and short timescales. *J. Atmos. Sci.*, **41**, 961–979.
- , —, —, and H.-H. Su, 1984b: Time variation of 500-mb height fluctuations with long, intermediate, and short timescales as introduced from lag-correlation statistics. *J. Atmos. Sci.*, **41**, 981–991.
- Chang, E. K. M., 1993: Downstream development of baroclinic waves as inferred from regression analysis. *J. Atmos. Sci.*, **50**, 2038–2053.
- Chang, H.-R., and P. J. Webster, 1990: Energy accumulation and emanation at low latitudes. Part II: Nonlinear response to strong episodic equatorial forcing. *J. Atmos. Sci.*, **47**, 2624–2644.
- , and —, 1995: Energy accumulation and emanation at low latitudes. Part III: Forward and backward accumulation. *J. Atmos. Sci.*, **52**, 2384–2403.
- Charney, J. G., 1963: A note on large-scale motions in the Tropics. *J. Atmos. Sci.*, **20**, 607–609.
- Davidson, N. E., and H. H. Hendon, 1989: Downstream development in the Southern Hemisphere monsoon during FGGE/WMONEX. *Mon. Wea. Rev.*, **117**, 1458–1470.
- Dunkerton, T. J., 1993: Observation of 3–6-day meridional wind oscillations over the tropical Pacific, 1973–1992: Vertical structure and interannual variability. *J. Atmos. Sci.*, **50**, 3292–3307.
- , and M. P. Baldwin, 1995: Observation of 3–6-day meridional wind oscillations over the tropical Pacific, 1973–1992: Horizontal structure and propagation. *J. Atmos. Sci.*, **52**, 1585–1601.

- Emanuel, K. A., 1991: The theory of hurricanes. *Annu. Rev. Fluid Mech.*, **23**, 179–196.
- , 1993: The effect of convective response time on WISHE modes. *J. Atmos. Sci.*, **50**, 1763–1775.
- , J. D. Neelin, and C. S. Bretherton, 1994: On large-scale circulations in convecting atmospheres. *Quart. J. Roy. Meteor. Soc.*, **120**, 1111–1143.
- Farrell, B., and I. Watterson, 1985: Rossby waves in opposing currents. *J. Atmos. Sci.*, **42**, 1746–1756.
- Ferreira, R. N., and W. H. Schubert, 1997: Barotropic aspects of ITCZ breakdown. *J. Atmos. Sci.*, **54**, 261–285.
- Flierl, G. R., M. E. Stern, and J. A. Whitehead Jr., 1983: The physical significance of modons: Laboratory experiments and general integral constraints. *Dyn. Atmos. Oceans*, **7**, 233–263.
- Gray, W. M., 1979: Hurricanes: Their formation, structure and likely role in the tropical circulation. *Meteorology over the Tropical Oceans*, D. B. Shaw, Ed., Royal Meteorological Society, 155–218.
- Heta, Y., 1991: The origin of tropical disturbances in the equatorial Pacific. *J. Meteor. Soc. Japan*, **69**, 337–351.
- Holland, G. J., 1995: Scale interaction in the western Pacific monsoon. *Meteor. Atmos. Phys.*, **56**, 57–79.
- Holton, J. R., 1970: A note on forced equatorial waves. *Mon. Wea. Rev.*, **98**, 614–615.
- , 1971: A diagnostic model for equatorial wave disturbances: The role of vertical shear of the mean zonal wind. *J. Atmos. Sci.*, **28**, 55–64.
- , 1992: *An Introduction to Dynamic Meteorology*. Academic Press, 511 pp.
- Hoskins, B. J., I. N. James, and G. H. White, 1983: The shape, propagation and mean-flow interaction of large-scale weather systems. *J. Atmos. Sci.*, **40**, 1595–1612.
- Kalnay, E., and Coauthors, 1996: The NCEP/NCAR 40-Year Reanalysis Project. *Bull. Amer. Meteor. Soc.*, **77**, 437–471.
- Kung, E. C., and L. P. Merritt, 1974: Kinetic energy sources in large-scale tropical disturbances over the Marshall Islands area. *Mon. Wea. Rev.*, **102**, 489–502.
- Lau, K.-H., 1991: An observational study of tropical summertime synoptic scale disturbances. Ph.D. thesis, Princeton University, 243 pp.
- , and N.-C. Lau, 1990: Observed structure and propagation characteristics of tropical summertime synoptic scale disturbances. *Mon. Wea. Rev.*, **118**, 1888–1913.
- , and —, 1992: The energetics and propagation dynamics of tropical summertime synoptic-scale disturbances. *Mon. Wea. Rev.*, **120**, 2523–2539.
- Liebmann, B., and H. H. Hendon, 1990: Synoptic-scale disturbances near the equator. *J. Atmos. Sci.*, **47**, 1463–1479.
- Lighthill, J., 1978: *Waves in Fluids*. Cambridge University Press, 504 pp.
- Lim, G. H., and J. M. Wallace, 1991: Structure and evolution of baroclinic waves as inferred from regression analysis. *J. Atmos. Sci.*, **48**, 1718–1732.
- McBride, J. L., and R. Zehr, 1981: Observational analysis of tropical cyclone formation. Part II: Comparison of non-developing versus developing systems. *J. Atmos. Sci.*, **38**, 1132–1151.
- McWilliams, J. C., P. R. Gent, and N. J. Norton, 1986: The evolution of balanced, low-mode vortices on the β -plane. *J. Phys. Oceanogr.*, **16**, 838–855.
- Molinari, J., D. Knight, M. Dickinson, D. Vollaro, and S. Skubis, 1997: Potential vorticity, easterly waves, and eastern Pacific tropical cyclogenesis. *Mon. Wea. Rev.*, **125**, 2699–2708.
- Mozer, J. B., and J. A. Zehnder, 1996: Lee vorticity production by large-scale tropical mountain ranges. Part I: Eastern North Pacific tropical cyclogenesis. *J. Atmos. Sci.*, **53**, 521–538.
- Nitta, T., 1970: A study of generation and conversion of eddy available potential energy in the tropics. *J. Meteor. Soc. Japan*, **48**, 524–528.
- , 1972: Energy budget of wave disturbances over the Marshall Islands during the years of 1956 and 1958. *J. Meteor. Soc. Japan*, **50**, 71–84.
- , and M. Yanai, 1969: A note on the barotropic instability of the tropical easterly current. *J. Meteor. Soc. Japan*, **47**, 127–130.
- , and Y. Takayabu, 1985: Global analysis of the lower tropospheric disturbances in the tropics during the northern summer of the FGGE year. Part II: Regional characteristics of the disturbances. *Pure Appl. Geophys.*, **123**, 272–292.
- Plumb, R. A., 1986: Three-dimensional propagation of transient quasi-geostrophic eddies and its relationship with the eddy forcing of the time-mean flow. *J. Atmos. Sci.*, **43**, 1657–1678.
- Raymond, D. J., and H. Jiang, 1990: A theory for long-lived mesoscale convective systems. *J. Atmos. Sci.*, **47**, 3067–3077.
- , C. López-Carillo, and L. L. Cavazos, 1998: Case studies of developing east Pacific easterly waves. *Quart. J. Roy. Meteor. Soc.*, **124**, 2005–2034.
- Reed, R. J., and E. E. Recker, 1971: Structure and properties of synoptic-scale wave disturbances in the equatorial western Pacific. *J. Atmos. Sci.*, **28**, 1117–1133.
- , and R. H. Johnson, 1974: The vorticity budget of synoptic-scale wave disturbances in the tropical western Pacific. *J. Atmos. Sci.*, **31**, 1784–1790.
- Riehl, H., 1948: On the formation of typhoons. *J. Meteor.*, **5**, 247–264.
- Ritchie, E. A., and G. J. Holland, 1997: Scale interactions during the formation of typhoon Irving. *Mon. Wea. Rev.*, **125**, 1377–1396.
- Rotunno, R., and K. A. Emanuel, 1987: An air–sea interaction theory for tropical cyclones. Part II: Evolutionary study using a non-hydrostatic axisymmetric numerical model. *J. Atmos. Sci.*, **44**, 542–561.
- Sadler, J. C., 1976: A role of the tropical upper tropospheric trough in early season typhoon development. *Mon. Wea. Rev.*, **104**, 1266–1278.
- Schubert, W. H., P. E. Ciesielski, D. E. Stevens, and H.-C. Kuo, 1991: Potential vorticity modeling of the ITCZ and the Hadley circulation. *J. Atmos. Sci.*, **48**, 1493–1509.
- Shapiro, L. J., 1977: Tropical storm formation from easterly waves: A criterion for development. *J. Atmos. Sci.*, **34**, 1007–1021.
- , 1978: The vorticity budget of a composite African tropical wave disturbance. *Mon. Wea. Rev.*, **106**, 806–817.
- Skubis, S. T., D. Vollaro, and J. Molinari, 1997: Ray tracing of easterly wave packets. Preprints, *22d Conf. on Hurricanes and Tropical Meteorology*, Fort Collins, CO, Amer. Meteor. Soc., 662–663.
- Stevens, D. E., 1979: Vorticity, momentum, and divergence budgets of synoptic-scale wave disturbances in the tropical eastern Atlantic. *Mon. Wea. Rev.*, **107**, 535–550.
- , and R. S. Lindzen, 1978: Tropical wave-CISK with a moisture budget and cumulus friction. *J. Atmos. Sci.*, **35**, 940–961.
- , —, and L. J. Shapiro, 1977: A new model of tropical waves incorporating momentum mixing by cumulus convection. *Dyn. Atmos. Oceans*, **1**, 365–425.
- Tai, K.-S., and Y. Ogura, 1987: An observational study of easterly waves over the eastern Pacific in northern summer using FGGE data. *J. Atmos. Sci.*, **44**, 339–361.
- Takayabu, Y. N., 1994: Large-scale cloud disturbances associated with equatorial waves. Part I: Spectral features of the cloud disturbances. *J. Meteor. Soc. Japan*, **72**, 433–449.
- , and M. Murakami, 1991: The structure of super cloud clusters observed in 1–20 June 1986 and their relationship to easterly waves. *J. Meteor. Soc. Japan*, **69**, 105–125.
- , and T. Nitta, 1993: 3–5 day period disturbances coupled with convection over the tropical Pacific Ocean. *J. Meteor. Soc. Japan*, **71**, 221–246.
- Thorncroft, C. D., and B. J. Hoskins, 1994: An idealized study of African easterly waves. I: A linear view. *Quart. J. Roy. Meteor. Soc.*, **120**, 953–982.
- Wallace, J. M., 1971: Spectral studies of tropospheric wave disturbances in the tropical western Pacific. *Rev. Geophys. Space Phys.*, **9**, 557–611.
- , G.-H. Lim, and M. L. Blackmon, 1988: Relationship between

- cyclone tracks, anticyclone tracks, and baroclinic waveguides. *J. Atmos. Sci.*, **45**, 439–462.
- Webster, P. J., and H.-R. Chang, 1988: Equatorial energy accumulation and emanation regions: Impacts of a zonally varying basic state. *J. Atmos. Sci.*, **45**, 803–829.
- Yanai, M., 1964: Formation of tropical cyclones. *Rev. Geophys.*, **2**, 367–414.
- , and M. M. Lu, 1983: Equatorially trapped waves at the 200 mb level and their association with meridional convergence of wave energy flux. *J. Atmos. Sci.*, **40**, 2785–2803.
- Young, W. R., and P. B. Rhines, 1980: Rossby wave action, enstrophy and energy in forced mean flows. *Geophys. Astrophys. Fluid Dyn.*, **15**, 39–52.
- Zangvil, A., and M. Yanai, 1980: Upper tropospheric waves in the Tropics. Part I: Dynamical analysis in the wavenumber-frequency domain. *J. Atmos. Sci.*, **37**, 283–298.
- Zehr, R. M., 1992: Tropical cyclogenesis in the western north Pacific. NOAA Tech. Rep. NESDIS 61, 181 pp. [Available from U.S. Department of Commerce, NOAA/NESDIS, 5200 Auth Rd., Washington, DC 20233.]